Impact of Heavy Aircraft Operations on Airport Capacity at Newark Liberty International Airport

Ioannis Simaiakis,* Alexander D. Donaldson† and Hamsa Balakrishnan‡

Massachusetts Institute of Technology, Cambridge, MA 02139, USA

Aviation System Performance Metrics (ASPM) departure and arrival rate data is collected for four common airport configurations at Newark Liberty International Airport (EWR) under Visual Meteorological Conditions (VMC) for the period 2007-2008. The effect of the number of Heavy (including Boeing 757) operations on overall airport throughput is then investigated. The investigation shows that Heavy departures and arrivals negatively impact overall airport capacity. Mechanisms by which controllers mitigate the effects of Heavy arrivals and departures are also identified. A preliminary quantification of the impact of operations of Heavy aircraft is performed with a parametric estimation of the capacity of the airport. The findings of this empirical study highlight that Heavy aircraft departures introduce a very small efficiency loss in terms of airport departure capacity. By contrast, under some runway configurations, Heavy aircraft arrivals have a more detrimental effect on airport departure capacity.

Acronyms

ASPM Aviation System Performance Metrics

EWR Newark Liberty International Airport

FAA Federal Aviation Administration

IMC Instrument Meteorological Conditions

JFK New York John F. Kennedy International Airport

LGA New York LaGuardia Airport

MTOW Maximum Takeoff Weight

ROT Runway Occupancy Time

VMC Visual Meteorological Conditions

I. Introduction

Accurately quantifying the number of arrivals and departures possible at an airport is important for both strategic planning purposes and tactical air traffic management. The capacity of an airport is defined as the maximum number of arrival and departures possible at a given time and varies due to a wide range

*PhD Candidate, Department of Aeronautics and Astronautics, Massachusetts Institute of Technology, Cambridge, MA 02139. ioa_sim@mit.edu. AIAA Student Member.

†PhD Candidate, Department of Aeronautics and Astronautics, Massachusetts Institute of Technology, Cambridge, MA 02139. alexdon@alum.mit.edu. AIAA Student Member.

‡Assistant Professor, Department of Aeronautics and Astronautics, Massachusetts Institute of Technology, Cambridge, MA 02139. hamsa@mit.edu. AIAA Senior Member.

of environmental and operational factors. Typically, the ratio of arrivals to departures is assumed to be the primary factor influencing airport capacity. Little consideration is given to the limitations on capacity imposed by the different mix of aircraft types operating at the airport. The aircraft types affect airport capacity because larger aircraft generally require greater in-trail spacing than smaller types, in order to safely separate following aircraft from their wake vortices.

This study will first demonstrate the impact of Heavy aircraft arrival and departure rates on the capacity envelope at Newark Liberty International Airport (EWR) and then develop a method to quantify that impact. The aim of this study is to demonstrate the influence of aircraft size on airport capacity, using EWR as a case-study.

II. Background

Airport capacity analysis plays an important role in the management of traffic flows at airports. Due to this importance, airport capacity airport capacity is quantified through both empirical[10] and theoretical[2] methods. The capacity of an airport varies with time through the influence of many different factors. Any quantification of airport capacity must be simple enough to be used for planning purposes, yet also sufficiently detailed to capture the major factors influencing capacity.

A. Airport Capacity Representation

A method for empirically deriving the capacity envelope of an airport was first proposed by Gilbo.[10] This capacity estimation method rejects outliers using statistical confidence bounds, to provide a more robust estimate of the airport capacity. The paper, however, does not address the possible cause of variations in the achieved throughput. Figure 1 shows an example capacity envelope for EWR based on 2007-2008 capacity measurement for one configuration, without filtering any outliers. Figure 1 also shows the sensitivity of the envelope to the low frequency data points. The hypothesis investigated in this study is that some of the variability seen in the airport capacity is due to differences in the mix of aircraft operating for different measurement periods. This effect is caused by differences in aircraft performance as well as separation rules for different aircraft types, impacting the throughput of both arrival and departure runways.

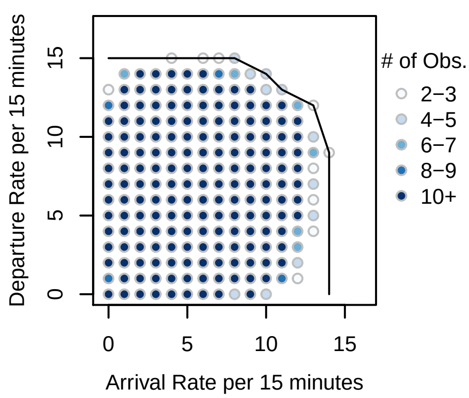

Figure 1: An example capacity envelope for EWR for the configuration using 22L for arrivals and 22R for departures.

B. Wake Vortex Separation Requirements

Runway capacity is dictated by the required spacing between subsequent operations. These separation requirements are determined by the operating procedures used by air traffic control. They are designed to ensure that aircraft are protected from the aircraft ahead of them. In the US, aircraft are grouped into five categories based on Maximum Takeoff Weight (MTOW) for the purposes of wake vortex separation,[5,9] as shown in Table 1.

Table 1: FAA aircraft wake categories and required departure separations.

Wake Category	MTOW (lb)	-or-	Aircraft Type	Separation after departure (minutes)
Small (S)	$< 41,000$			Not specified
Large (L)	$41,000 - 255,000$			Not specified
Boeing 757 (B757)			Boeing 757 Series	2
Heavy (H)	$> 255,000$			2
Super (J)			Airbus A380 Series	3

Table 1 shows that the separation rules for departing aircraft depend only on the weight class of the lead departure, and are not explicitly defined for Small and Large aircraft. In contrast, the required spacing between two arrivals depends on the category of both the leading and trailing aircraft which results in the more complex set of separation rules shown in Table 2.

Table 2: FAA-mandated separation between pairs of arriving aircraft.

Separation (NM)	Trailing aircraft type				
Leading aircraft type	Super	Heavy	B757	Large	Small
Super	6	6	8	8	10
Heavy	R[a]	4	5	5	6
B757	R[a]	4	4	4	5
Large	R[a]	R[a]	R[a]	R[a]	4
Small	R[a]	R[a]	R[a]	R[a]	R[a]

[a] R denotes application of standard terminal radar separation, which is 2.5 n.m. at EWR.

C. Newark Liberty International Airport

EWR is the focus of this study due to the simplicity of its runway layout, relatively frequent Heavy aircraft movements, and high overall traffic levels. The airport has two long, closely-spaced main parallel runways (4L/22R and 4R/22L) as well as a shorter crossing runway, 11/29 that intersects both the main runways close to their northern thresholds. Under typical operating conditions 4L/22R is used for departures and 4R/22L for arrivals. Runway 11/29 is used for arrivals as required during high traffic periods; however, use of this runway is typically restricted to aircraft smaller than a 737-700, and it is therefore not routinely used by Heavy aircraft. The direction of operation on the main runways is dictated by wind direction and velocity, with takeoffs and landings being conducted into the wind. While unusual wind conditions may require more extensive use of the crossing runway, these low-capacity configurations are avoided whenever possible. This study will focus on the four most common configurations of EWR, as shown in Figure 2.

The distribution of Heavy aircraft operations during different hours of the day is shown in Figure 3. We note that Heavy aircraft arrival and departure rates at EWR are typically fewer than three per 15-minute interval. The Heavy departure rate is higher during the 5-8 p.m. period due to the increased international departure traffic during this time. Heavy arrivals tend to be slightly higher in the 11 a.m.-4 p.m. period preceding the evening Heavy departure activity. Substantially higher rates of Heavy operations also occur occasionally, as demonstrated by the long tails in the distributions shown in Figure 3.

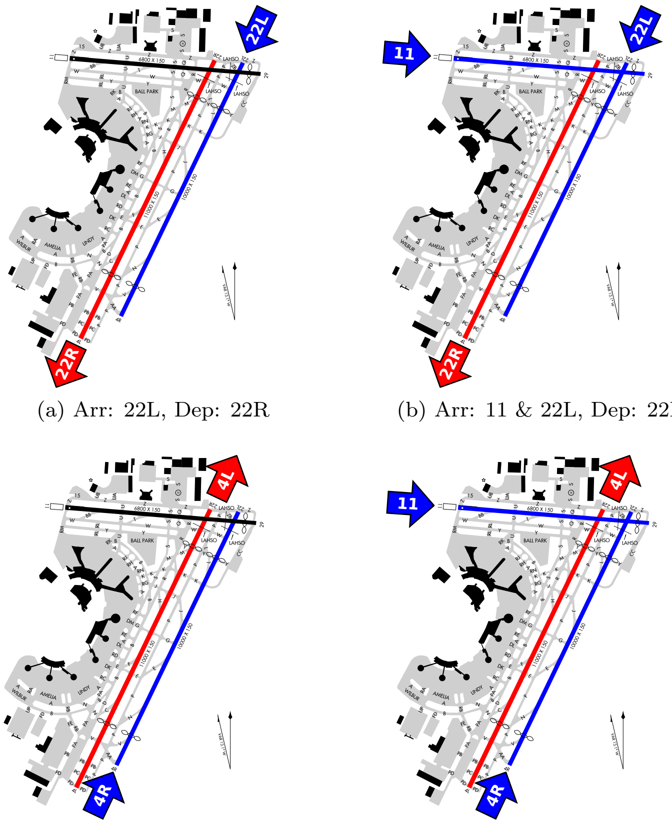

(a) Arr: 22L, Dep: 22R

(b) Arr: 11 & 22L, Dep: 22R

(c) Arr: 4R, Dep: 4L

(d) Arr: 4R & 11, Dep: 4L

Figure 2: The four EWR runway configurations examined in this analysis.

III. Capacity Envelope Analysis

In this section, we will extend traditional capacity envelope analysis techniques to include Heavy aircraft arrival and departure rates. These Heavy aircraft operations are a potential explanatory variable that could account for some of the variability observed in achieved airport capacities. Section IV will provide a rigorous technique for quantifying these effects.

A. Methodology

Every flight arriving or departing from EWR during the period 2007-2008 was extracted from the Aviation System Performance Metrics (ASPM) "individual flights" database.[7] This database provided the arrival or departure times well as the type of aircraft for each flight. Each flight was assigned the appropriate wake vortex category, by using the FAA aircraft characteristics database[6] to find the MTOW of the flight based on the aircraft type, and determining the appropriate wake vortex category as described in II.B. The number of arrivals and departures for each wake category, as well as the total number of arrivals and departures, were then calculated for each quarter hour period.

The quarter-hourly operation counts were then merged with airport runway configuration and weather information from the ASPM airport configuration database. In this initial study, operations were grouped further by combining the Boeing 757 and Heavy wake categories. For departures this combination is unlikely to be a source of significant error, because the Boeing 757 and Heavy categories have the same departure separation requirements (as shown in Table 1). For arrivals, however, this is an oversimplification of the separation standards: separation requirements for arrivals depend on both the lead and following aircraft

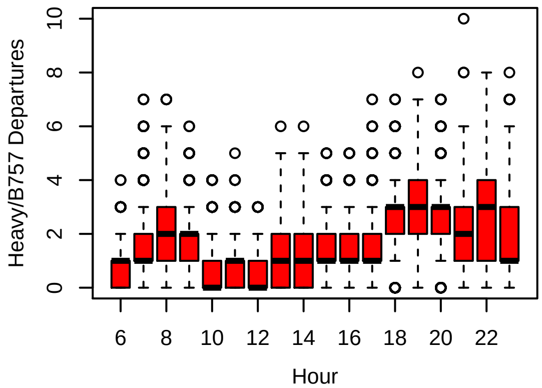

(a) Departures

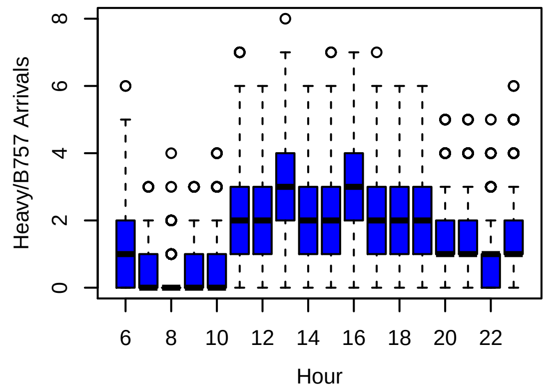

(b) Arrivals

Figure 3: Box-plots showing the distribution of Heavy and Boeing 757 operations throughout the day at EWR for the period 2007-2008.

categories, and the effect of the aircraft sequence in each period would have to be examined. While such a study would provide interesting insight into how the airport optimizes the arrival stream, it is beyond the scope of this analysis. Therefore, this study will focus on the effect of Heavy (including Boeing 757) *departures* on airport capacity.

In order to control for the effects of runway configuration and meteorological conditions, the airport capacity measurement was performed individually for different runway configurations. The analysis was also limited to daytime[a] operations under Visual Meteorological Conditions (VMC), which occur 84% of the time. During these daytime VMC periods, four runway configurations account for 91% of the measurements, as shown in Table 3. The effect of Heavy aircraft operations will be measured for these four common configurations.

Table 3: Frequency of use of studied EWR configurations under Visual and Instrument Meteorological Conditions.

		VMC		IMC	
Arrival Runway(s)	Departure Runway	Count	Frequency	Count	Frequency
22L	22R	17810	40.3%	3322	40.0%
11, 22L	22R	8131	18.4%	297	3.6%
4R	4L	9476	21.5%	3924	47.2%
4R, 11	4L	4620	10.5%	344	4.1%

B. Results

Each point in Figure 4 represents the airport throughput during a 15-minute interval that was observed sometime during the two year measurement period. The color of the points represents the maximum number of Heavy (and Boeing 757) departures observed for that particular value of throughput. These plots show a clear trend towards lower levels of Heavy departures at the edge of the capacity envelope. This observation reflects the larger separations required after Heavy departures. The capacity envelopes also suggest that Heavy departures have a greater effect on arrival capacity than they do on departure capacity. This larger effect on arrivals was unexpected, because departure and arrival operations occur on different runways in all of the studied configurations.

[a]Defined as operations occurring between 6 a.m. and 12 a.m.

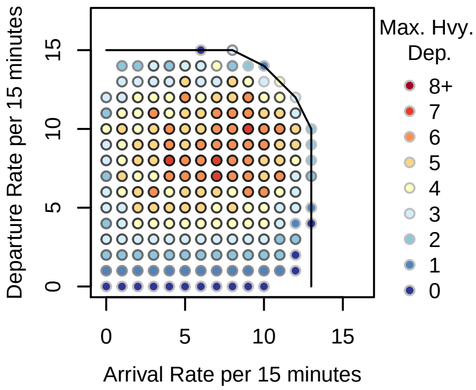

(a) Arr: 22L, Dep: 22R

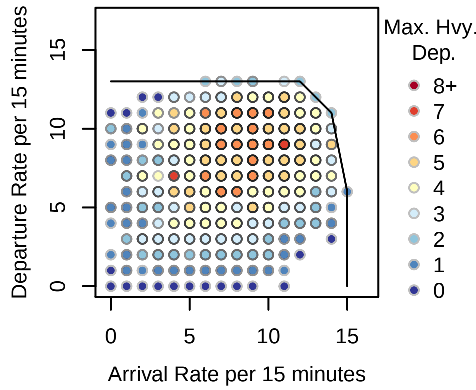

(b) Arr: 11 & 22L, Dep: 22R

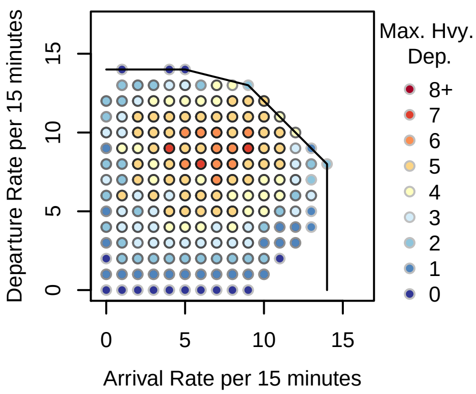

(c) Arr: 4R, Dep: 4L

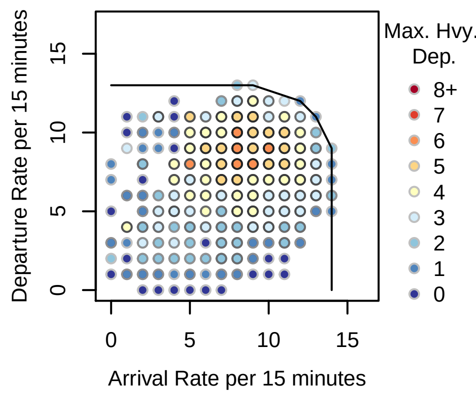

(d) Arr: 4R & 11, Dep: 4L

Figure 4: Capacity envelopes for the four studied configurations colored to show the maximum number of Heavy departures at each operating point.

1. Effect of Heavy Departures on Arrival Capacity

Due to arrival and departure operations occurring on separate runways, the impact of Heavy departures on arrival throughput was expected to be minimal. However, the initial analysis shown in Figure 5 suggests that this is not the case. Increased Heavy aircraft departure rates are associated with a lower total arrival throughput at the airport. This correlation may simply be due to high Heavy departure rates corresponding to high levels of total departures at the airport, which are known to impact arrival rates (as seen in Figure 1). The effect could also be due to interactions specific to Heavy Departures. The statistical analysis technique described in Section IV will be used to investigate these possibilities.

2. Effect of Heavy Departures on Departure Capacity

Because the four configurations studied each use one primary departure runway, a strong negative correlation between the Heavy aircraft departure rate and total departure would be expected. Such a relationship would arise because Heavy departures require more than twice the time separation required by Large or Small aircraft. As expected, Figure 6 shows such a negative correlation between Heavy aircraft departure rate and overall departure rate. The slope of the curve in the trade-off region is approximately -1 in all cases, suggesting that each Heavy departure from a runway reduces the total departure capacity of the runway by one "average" operation. This is the ratio that would be expected from the two-minute wake separation requirement, if a non-Heavy operation required approximately one-minute of Runway Occupancy Time (ROT), or the time required to ensure the 2.5 NM terminal radar separation. However, the trade-off region starts only after 2-4 Heavy aircraft departures, suggesting that a modest number of Heavy aircraft in

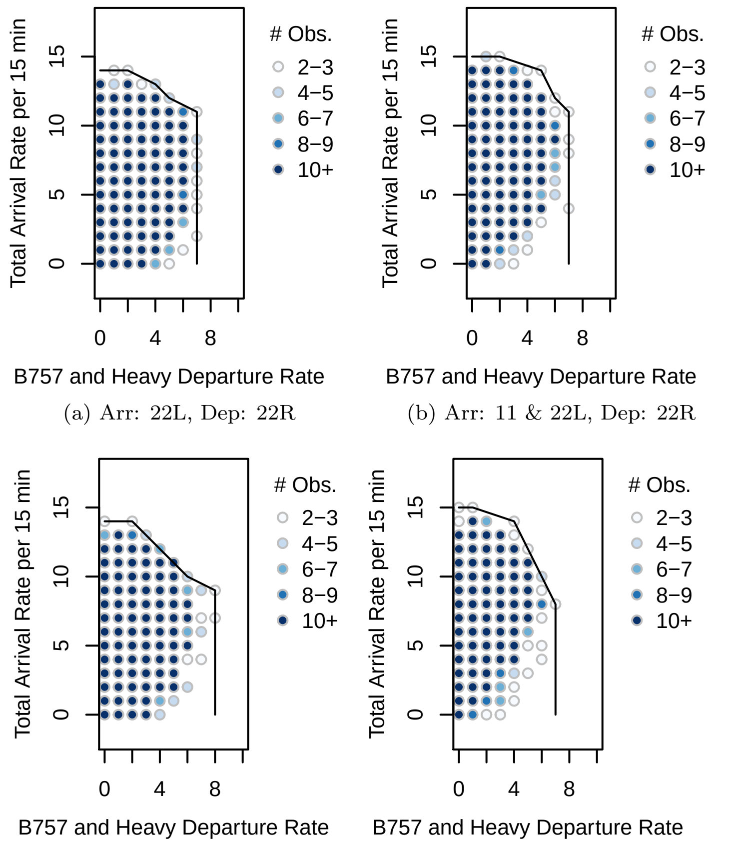

(a) Arr: 22L, Dep: 22R
(b) Arr: 11 & 22L, Dep: 22R
(c) Arr: 4R, Dep: 4L
(d) Arr: 4R & 11, Dep: 4L

Figure 5: Envelopes showing the relationship between Heavy departures and total arrival capacity at EWR.

the fleet mix may not impact the total departure rate.

3. *Effect of Heavy Arrivals on Departure Capacity*

A tradeoff between the Heavy arrival rate and total departure rate was not expected due to the segregation of arrivals and departures for the configurations analysed. However, Figure 7 shows that contrary to these expectations, Heavy arrival volume does appear to have a significant detrimental impact on departure rate. This could either be due to either Heavy arrivals requesting the departure runway[b] or the additional time required for Heavy arrivals to cross the departure runway. Heavy arrivals crossing the departure runway disrupt the flow of departing traffic because Heavy aircraft accelerate slowly while taxiing. Controllers therefore either have Heavy aircraft exit the arrival runway and immediately cross the departure runway without slowing down, or else have to bring the Heavy aircraft to a full stop before crossing the departure runway. Both maneuvers disrupt the departure flow.

IV. Quantification of the Impact of Heavy Aircraft Operations

In this section, we focus on quantifying the impact of the Heavy operations on airport throughput, which was qualitatively analyzed in Section III. We demonstrate the methodology by analyzing runway configuration (4R | 4L). In the next section, we apply the same method to the other two major runway configurations. Our methodology focuses on parametrically estimating and representing the departure capacity of the runway

[b]This runway may be requested for reasons of safety by pilots because it is 1000 ft longer than the arrival runway

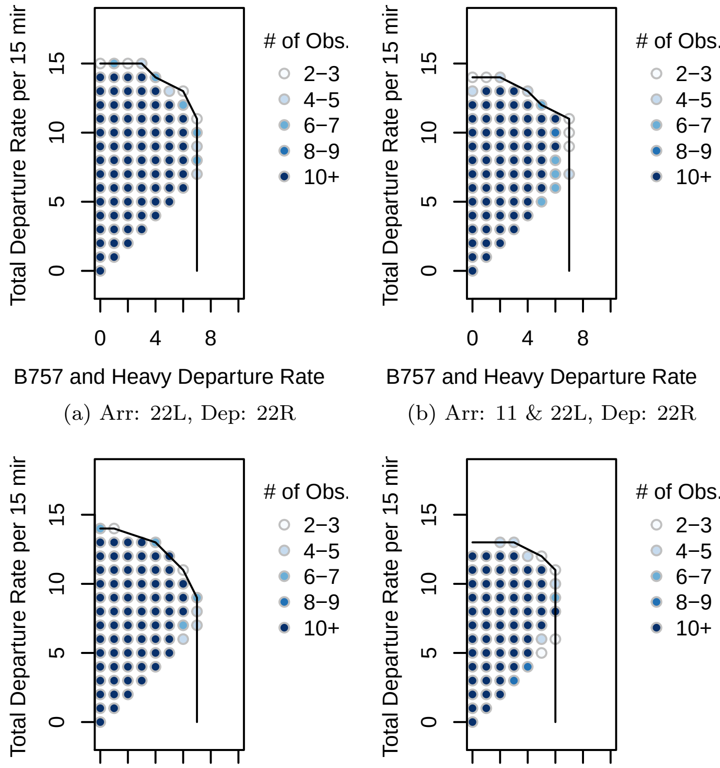

(a) Arr: 22L, Dep: 22R

(b) Arr: 11 & 22L, Dep: 22R

(c) Arr: 4R, Dep: 4L

(d) Arr: 4R & 11, Dep: 4L

Figure 6: Envelopes showing the relationship between Heavy departures and total departure capacity at EWR.

system. For the purposes of this work, the departure capacity of the runway system is defined as the average number of departures that can be performed on the runway system in the presence of persistent demand conditioned on relevant parameters, such as landings, runway crossings, Heavy aircraft operations, etc. All estimation problems are formulated as convex optimization problems extending the methodology analyzed in earlier work,[17] and are solved using `CVX`, a package for specifying and solving convex programs.[11,12]

A. Average Departure Throughput

The starting point for the departure throughput estimation is the representation of the departure throughput (or takeoff rate) as a function of departure demand. The departure demand, $N(t)$, at some time t (represented in 1-minute increments) is measured as the number of aircraft taxiing out during that time interval. In other words, it is the number of aircraft that have pushed back but have not yet taken off. The departure throughput during a 15-minute period starting at time t is defined as the takeoff rate $\bar{T}(t)$ over this time period, and is measured as the number of aircraft that took off during the 15-minute interval $[t, t+15)$.

This representation yields the plots in Figure 8a for the runway configuration 4R | 4L at EWR in 2007 under VMC. For the entire year, we have 86,942 data points, $(N, \bar{T})$. In Figure 8a, we plot the mean and median takeoff rate for each value of the departure demand, N. The error bars depict the standard deviation of the takeoff rate at each value of N.

As $N(t)$ increases, the takeoff rate initially increases, but then saturates at a critical value N^*. From Figure 8a, we can infer that the average takeoff rate in saturation is around 10 to 11 aircraft/15 minutes. The critical value, N^*, is difficult to determine visually, because the mean and median throughput appear

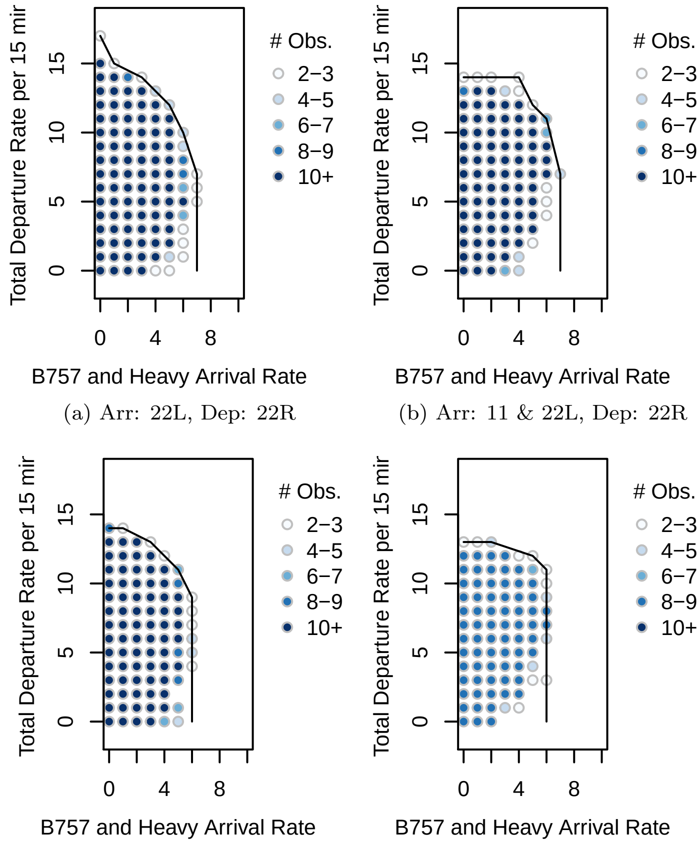

(a) Arr: 22L, Dep: 22R
(b) Arr: 11 & 22L, Dep: 22R
(c) Arr: 4R, Dep: 4L
(d) Arr: 4R & 11, Dep: 4L

Figure 7: Envelopes showing the relationship between Heavy arrivals and total departure capacity at EWR.

to saturate at different values.

We can formalize the estimation of the mean and median departure throughput as a function of the departure demand by formulating the estimation problem as a regression problem. The function f to be fitted has to conform to the physics of the system:

- Departure throughput is a monotonically non-decreasing function of departure demand.
- Departure throughput is a concave function of departure demand.

The estimation problem can be formulated as a least-squares problem: Given m pairs of measurements $(N(t), \bar{T}(t))$, denoted $(u_1, y_1), \ldots, (u_m, y_m)$, we seek a non-decreasing, concave function $f : \mathbb{R} \rightarrow \mathbb{R}$ that estimates the mean $\bar{T} = f(N)$. This infinite-dimensional problem gets significantly simplified by the fact that we have measurements only for discrete values of $N(t)$ and consequently, only discrete values of f. We need to estimate the points $f(0), f(1), \ldots, f(n)$, where $n = \max(N(t))$. The function f is therefore simply a piecewise linear function of N, and the monotonicity and concavity constraints are imposed at the points $0, 1, \ldots, \max(N(t))$ by comparing the values and the slopes of subsequent pieces. $\bar{T}$ is given by the solution

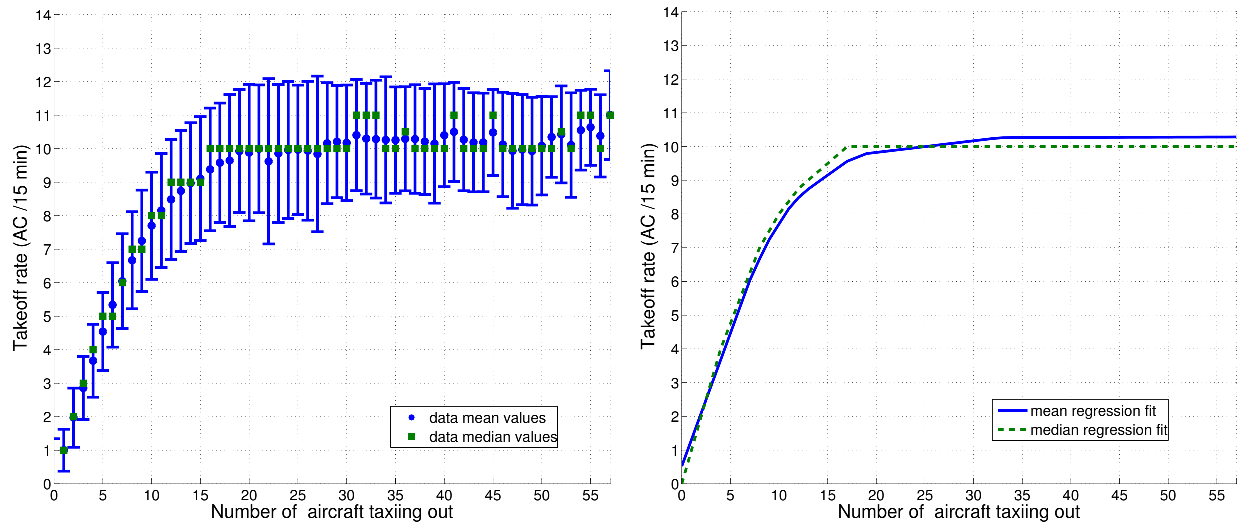

(a) Measurements of the takeoff rate as function of the number of aircraft taxiing out.

(b) Regression of the takeoff rate as function of the number of aircraft taxiing out.

Figure 8: EWR throughput of runway configuration (4R | 4L).

to the following convex optimization problem:

$$\min \sum_{i=1}^{m} (\hat{y}_i - y_i)^2 \tag{1}$$

subject to:

$$\hat{y}_i = f(u_i), \;\; i = 1, \ldots, m \tag{2}$$
$$f(i+1) \geq f(i), \;\; i = 0, \ldots (n-1) \tag{3}$$
$$f(i+1) - f(i) \leq f(i) - f(i-1), \;\; i = 1, \ldots (n-1) \tag{4}$$

Similarly, the median estimation problem is formulated as:

$$\min \sum_{i=1}^{m} |\hat{y}_i - y_i| \tag{5}$$

subject to:

$$\hat{y}_i = f(u_i), \;\; i = 1, \ldots, m \tag{6}$$
$$f(i+1) \geq f(i), \;\; i = 0, \ldots (n-1) \tag{7}$$
$$f(i+1) - f(i) \leq f(i) - f(i-1), \;\; i = 1, \ldots (n-1) \tag{8}$$

The results of the regression fit are shown in Figure 8b. The mean takeoff rate saturates at 10.25 aircraft/15 minutes when $N \geq 33$ and median takeoff rate saturates at 10 aircraft/15 minutes when $N \geq 17$. We can conclude that the average takeoff rate of this runway configuration under persistent demand is approximately 10 aircraft/15 minutes, or 40 takeoffs per hour. However, the results of the mean and the median fits do not seem to yield a consistent value of N^*, as the mean takeoff rate stabilizes when $N \geq 33$, whereas the median stabilizes when $N \geq 17$.

B. Estimation of the Saturation Point, N^*

Traditional statistical methods for the problem of predicting the response variable (departure throughput) as a function of several independent variables (departure demand, arrival throughput, fleet mix) would make it difficult for us to exploit the structure of the problem and to impose the constraints that result from the physics of the system. For this reason, we follow a different approach.

We isolate instances of high departure demand, and then estimate the departure throughput as a function of the arrival throughput and the fleet mix. To this end, we need to estimate the threshold N^* at which the departure throughput stops varying with departure demand. There are several ways to estimate N^*, for example through the inspection of Figure 8a or Figure 8b. However, the two curves of Figure 8b seem to suggest very different values for N^*.

A more robust way to identify N^* is to group the throughput observations of each value of N and use a non-parametric method to test for significant differences between the throughput observations of each group. More specifically we use the Kruskal-Wallis one-way analysis of variance. For the 4R|4L runway configuration, the test does not reject the null-hypothesis that the throughput observations at different values of N are drawn from the same distribution at both 0.05 and 0.1 significance levels for $N \geq 28$. However, it does reject the null hypothesis if we include more groups at lower values of N. The test implies that the measurements of throughput for different values of $N \geq 28$ are not significantly different. All else being equal, the departure throughput does not significantly change with departure demand at demand values greater than or equal to 28. In other words, $N^* = 28$. We can now isolate all data points for which $N \geq 28$ and study the explanatory power of other variables. The Kruskal-Wallis test yields a much higher value for N^* (i.e., 28) than the one at which the median throughput saturates (i.e., 17) because the variance of the throughput is much higher for $20 \leq N < 28$ than for higher values of N. This trend can also be seen in Figure 8a.

C. Capacity Estimation

As a first step, we use the data points for which $N \geq N^*$ to plot the average departure throughput as a function of arrival throughput, and estimate the least square fit of a concave non-increasing function to the data. Given k pairs of measurements $\bar{A}(t)$ and $\bar{T}(t)$, denoted $(v_1, y_1), \ldots, (v_k, y_k)$ at all times when $N \geq N^*$, we seek a non-increasing, concave function $h : \mathbb{R} \to \mathbb{R}$ that estimates the mean $\bar{T} = h(\bar{A}|N \geq N^*)$. Again, we only need to estimate the points $h(0), h(1), \ldots, h(l)$, where $l = \max(\bar{A}(t))$. The function h is therefore a piecewise linear function of A, and the monotonicity and concavity constraints are imposed at the points $0, 1, \ldots, l$ by comparing the values and the slopes of subsequent pieces. The formulation of this estimation problem is as follows:

$$\min \sum_{i=1}^{k} (\hat{y}_i - y_i)^2 \tag{9}$$

subject to:

$$\hat{y}_i = h(v_i), \;\; i = 1, \ldots, k \tag{10}$$

$$h(i+1) \leq h(i), \;\; i = 0, \ldots (l-1) \tag{11}$$

$$h(i+1) - h(i) \leq h(i) - h(i-1), \;\; i = 1, \ldots (l-1) \tag{12}$$

The scatterplot of the data-points to which the fitting is applied and the plot of the estimated function (in red) can be seen in Figure 9a. The plot of Figure 9a provides a robust estimate of the average departure throughput as a function of the arrival throughput under persistent departure demand ($N \geq N^*$). It can also be interpreted as a capacity plot for this runway configuration. Each point represents a departure capacity, given an arrival capacity. For example, for an arrival rate of 10 aircraft/15 minutes, the average departure throughput of this runway configuration under persistent departure demand is 10 aircraft/15 minutes. This data-point would imply a capacity of 20 movements per 15 minutes, or 80 movements per hour. These numbers are very close to the FAA estimates which place the capacity of this runway configuration at 80-81 movements per hour.[13]

There is no operational rationale that requires the departure capacity of this runway configuration to be a concave function of the arrival capacity. Arrivals crossing the departure runway disrupt the flow of departing traffic. This penalty of this disruption does not need to be a concave function of the number of crossings in a 15 minute interval. Thus, we can relax the concavity constraint. The plot of the resulting function can be seen in Figure 9a in blue. Clearly, the relaxed capacity plot is not significantly different from the concave one. The concavity constraint merely results in a smoothing of the observations.

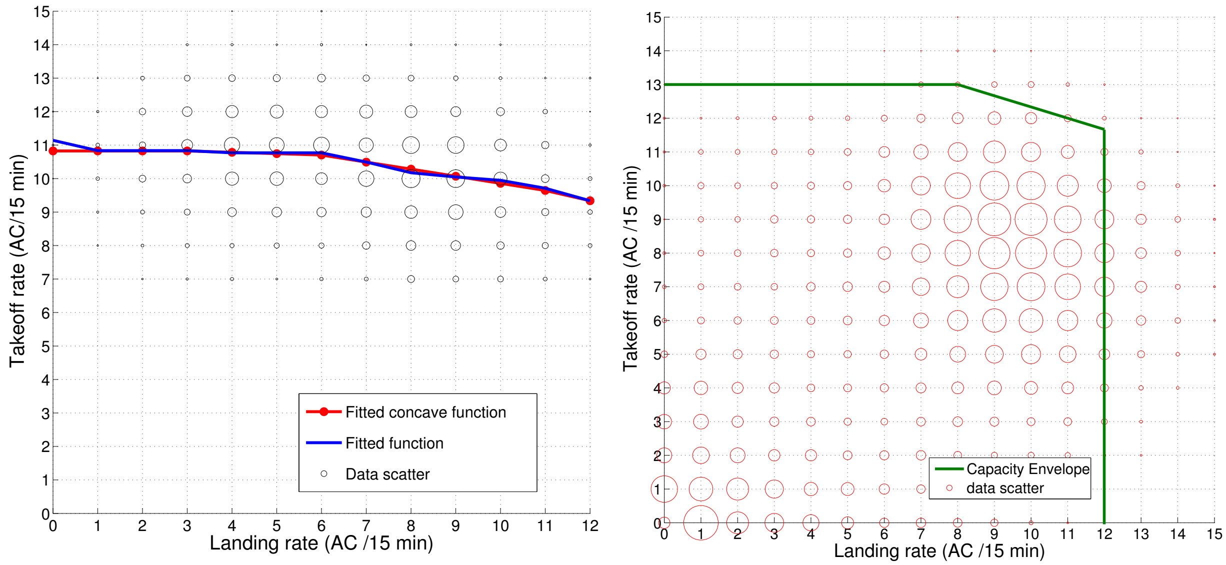

(a) Regression of the takeoff rate as function of landing rate when $N \geq N^*$.

(b) Capacity envelope.

Figure 9: Different measures of the capacity of the 4R|4L runway configuration of EWR.

It is logical to compare the estimated function plotted in Figure 9a to traditional empirical capacity envelope estimates. Empirical capacity envelopes represent the highest departure throughput as a concave non-increasing function of the arrival throughput. In other words, a capacity envelope is the convex hull enveloping all the observed maximum arrival and departure counts, after correcting for outliers. For the capacity envelope estimation, we use the approach suggested by Ramanujam and Balakrishnan,[15] which for this runway configuration at EWR yields the capacity envelope plotted in Figure 9b. The maximum total capacity is achieved at around 23-24 movements/ 15 minutes for several combinations of departures and arrivals. This number would translate to 92-96 operations per hour, which is much higher than the number of movements that this runway configuration can sustain.[13] This reveals an inherent ambiguity in the analysis of the capacity envelope. While the commonly accepted definition of capacity is "the *average* number of movements that can be performed on the runway system in the presence of continuous demand",[3] most empirical capacity envelope estimation methods focus on the best-case scenario, that is, the *maximum* number of movements that can be performed on the runway system. These maximum counts are achievable only under special circumstances, such as a favorable fleet mix or favorable sequencing. For this particular case, the difference between the *capacity envelope* and the *average departure throughput in the presence of continuous demand* estimates for the departure capacity at a given arrival throughput can be as large as 12 operations per hour.[c]

D. Analysis of the Impact of Fleet Mix on Capacity using Local Regression

In order to estimate the impact of fleet mix, we continue to work with the data points for which $N \geq N^*$. We address the problem of estimating the departure throughput as a function of the number of arrivals and the fleet mix. The fleet mix is not a simple numerical variable like the number of arrivals, and its impact is highly dependent on the particulars of each airport (such as, runway configuration, sequencing decisions, airspace design and local procedures). Following the analysis of Section III, our hypothesis is that the fleet mix can be represented with three variables:

- Number of Heavy aircraft ($HDeps$) taking off in the 15-minute interval.

[c]An extensive discussion of these different capacity metrics can be found in recent work of Pyrgiotis.[14]

- Number of Heavy aircraft ($HArrs$) landing in the 15-minute interval.[d]
- Number of propeller-powered aircraft or props ($PDeps$) taking off in the 15-minute interval.

The props clear the departure runway faster than larger aircraft, and thus could make runway crossings quicker and reduce the impact of arrivals.

We attempt to model the response variable, departure throughput (*Departures*) in each 15-minute time interval $[t, t + 15)$, as a function of four potential explanatory variables:

1. Number of departing aircraft on the ground at time t (*DepDem*)[e]
2. Number of landings in the 15 minute interval (*Arrivals*)
3. Number of props taking off in the 15-minute time interval ($PDeps$)
4. Number of Heavy aircraft taking off in the 15-minute time interval ($HDeps$)
5. Number of Heavy aircraft landing in the 15-minute time interval ($HArrs$)

We analyze the correlations between all the variables in the model, using the *pairs* function of the R programming language which produces panels with the correlations among the variables. Each panel in Figure 10 shows the scatterplot between the variable on the vertical axis and the variable on the horizontal axis as well as the lowess[f] curve, in red color, through a set of data points. Lowess fits follow the general trend of the data and so they are a good measure of the correlation between the two variables.[1] The response variable *Departures* is shown on the $y-$axis of the top row of the panels.

From Figure 10, we observe that:

- The lowess fit line for the variable pair (*DepDem*, *Departures*) does not exhibit any large or systematic deviance from the area between the $y = 10$ and $y = 11$ lines. This is further evidence that N^* was calculated robustly, and that for $N \geq N^*$, there is no correlation between the departure demand and the departure throughput. The departure throughput is shown to be stable at around 10.5 aircraft/15 min, similar to the value that was calculated using the estimation method of Figure 8b.
- The lowess fit line for the variable pair (*Arrivals*, *Departures*) follows the same trend as the curve of Figure 9a. It shows that the departure throughput drops from 11 to 9 operations as a concave function of the arrival throughput.
- The lowess fit line for the variable pair ($HDeps$, *Departures*) exhibits a decreasing trend. The curve decreases slowly from 11 to 10.
- The lowess fit line for the variable pair ($HArrs$, *Departures*) exhibit a clear negative correlation between the two. As the number of Heavy arrivals increases, the departure throughput decreases from 11 to a value of about 9.
- The lowess fit line for the variable pair ($PDeps$, *Departures*) does not show any correlation between the two.

The relationship between the departure throughput and these five variables is also examined with advanced statistical tools such as regression trees, random forests and generalized additive models. They all lead to the same conclusion: the three most significant explanatory variables are the arrivals, and the number of Heavy aircraft among both the arrivals and the departures.

[d]In the analysis from here on, we exclude B757s from the Heavy aircraft class, because B757s were shown to behave like Large aircraft with regard to departure throughput.

[e]Although we have established that the departure throughput does not change significantly with the number of aircraft on the ground, when $N \geq N^*$, it is useful to revisit this hypothesis in a more complex multi-variable model.

[f]locally weighted scatterplot smoothing

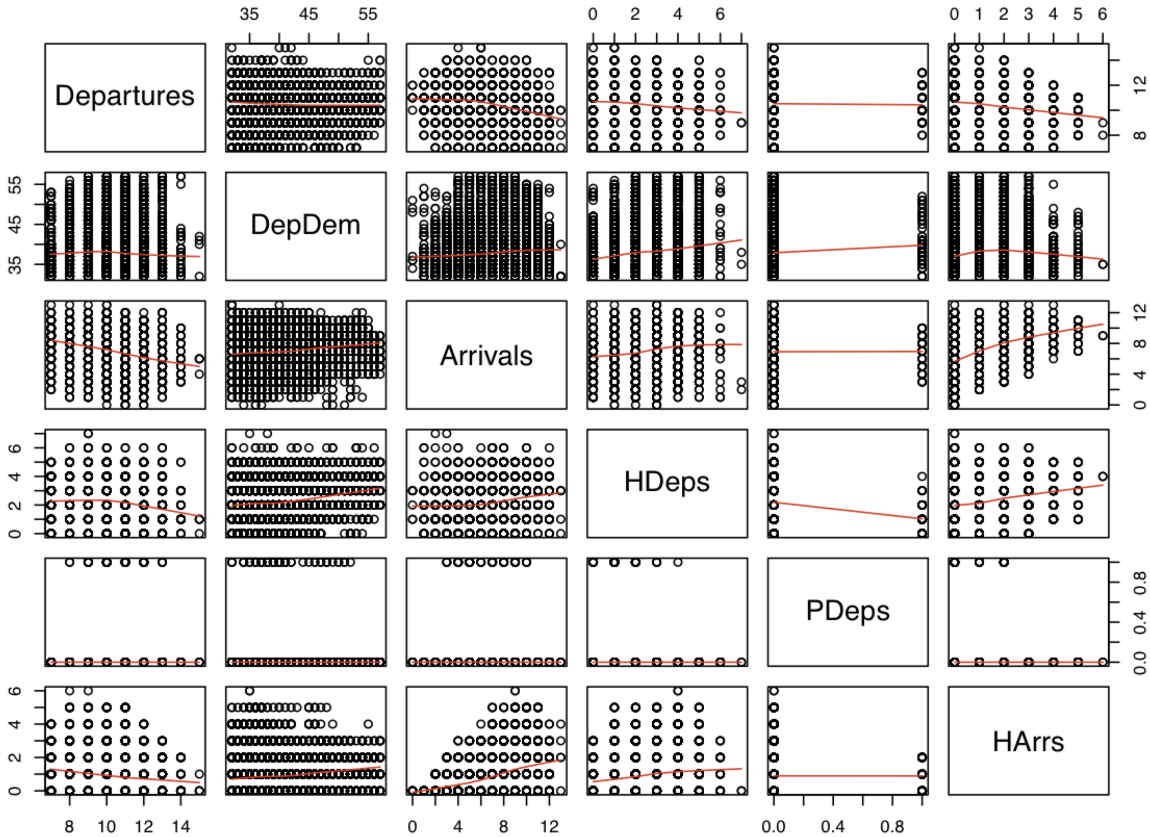

Figure 10: Correlations between departures, departure demand, arrivals, Heavy departures, prop departures and Heavy arrivals.

E. Parametric Representation of Departure Capacity

Having established that at $N \geq N^*$ the departure throughput is primarily a function of arrivals, Heavy arrivals and Heavy departures, we would like to estimate and represent this function. This is a challenging task because (1) it is hard to represent a three variable function, and (2) the impact of the explanatory variables is coupled. For these reasons, we adopt the approximative approach described in earlier work.[17] We first estimate the departure throughput under persistent demand as a function of the arrivals and the number of Heavy aircraft taking off in a 15-minute interval, neglecting the impact of Heavy arrivals. The plot of the estimated function, $h_1(\bar{A}, H_{Deps}|N \geq N^*)$, can be seen in Figure 11a overlaid with the red curve of Figure 9b (the *Average Fleet Mix Throughput*). The comparison shows that the lines in Figure 11a are in fact the red line parametrized by the number of Heavy aircraft taking off in the 15-minute interval.

We also estimate the departure throughput under persistent demand as a function of the arrivals and the number of Heavies landing in a 15-minute interval neglecting the impact of Heavy departures. The plot of the estimated function, $h_2(\bar{A}, H_{Arrs}|N \geq N^*)$, can be seen in Figure 11b overlaid with the red curve of Figure 9b (the *Average Fleet Mix Throughput*). The comparison shows that the solid lines in Figure 11b are in fact the red line parametrized by the number of Heavy arrivals.

From Figures 11a and 11b, we observe the following:

- The average departure throughput curve is close to that corresponding to a fleet mix of 2 Heavy aircraft taking off in a 15-minute interval. This is consistent with the number of Heavy aircraft in the fleet mix at EWR, which was around 22% in 2007.

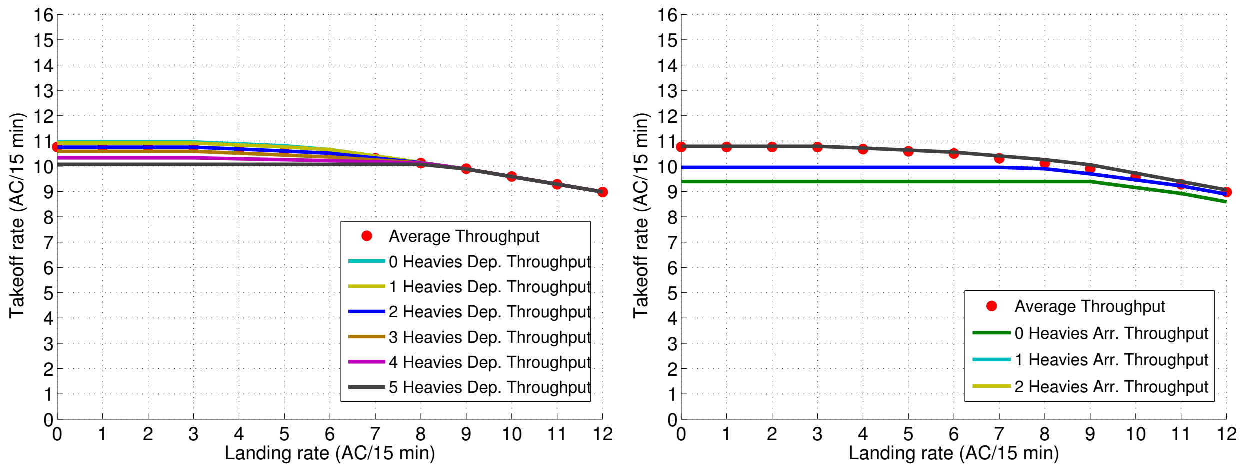

(a) Regression of the takeoff rate as function of landing rate and the number of Heavies departing when $N \geq N^*$.

(b) Regression of the takeoff rate as function of landing rate and the number of Heavies arriving when $N \geq N^*$.

Figure 11: Parametric representation of the capacity of the 4R|4L runway configuration.

- The number of Heavy aircraft that takeoff has a rather small impact on the departure throughput. For the most common operating scenarios in which the rate of arrivals is 5-10 aircraft/15-minutes and the number of Heavy aircraft is 1-3, the departure throughput does not change substantially.
- By contrast, the number of Heavy aircraft arrivals has a higher impact. For the most common operating scenarios in which the rate of arrivals is 5-10 aircraft/15-minutes, two Heavy arrivals reduce the departure throughput by between 0.5 and one operation (i.e., 2-4 operations per hour).
- As the number of arrivals increases, the impact of Heavy departures diminishes and all the curves collapse to a single one. This is likely because as the number of arrivals increases, the controllers use the increased spacing introduced by the Heavy departures to manage the runway crossings.
- Similarly, as the number of arrivals increases, the impact of Heavy arrivals decreases from more than 1 departure for 2 Heavies landing, to less than half a departure for two Heavies landing. An explanation for this could be that controllers use the extra time required for a Heavy arrival crossing to perform multiple crossings during arrival pushes. In this way, the impact of Heavy arrivals diminishes.
- A comparison of the curves of Figures 11a and 11b suggest that Heavy arrivals are more detrimental to departure throughput than Heavy departures. Two Heavy arrivals can introduce a departure throughput penalty of one operation per 15 minutes, whereas two Heavy departures do not reduce the departure efficiency.
- Finally, for low numbers of arrivals, and no Heavy aircraft in the fleet mix, the departure capacity is less than 11 takeoffs per 15 minutes. Theoretically, one would expect this number to be closer to 15[g]. The fact that it is significantly lower than the theoretical estimate suggests that other constraints (for example, TRACON capacity, En Route Center capacity, or traffic flow management programs) decrease the departure capacity of this runway configuration.

It is important to note that such a parametric representation assumes that there is no correlation between the Heavy departures and Heavy arrivals variables; an analysis of the relation between these variables is presented in Appendix A.

[g]The standard terminal radar separation between non-Heavy departures translates to approximately one minute separation between successive takeoffs with the same heading.

V. South Flow Configurations

In this section, we apply the methodology of Section IV to the two other major runway configurations of EWR, 22L|22R and 11,22L|22R. These configurations are primarily used under south winds.

As explained in Section C, runway 11 is added under high arrival demand. Several restrictions apply on its use due to its short length (6800 ft) and restricted approach geometry. Typically, use is limited to Boeing 737-700 and smaller aircraft and 15 miles spacing is required between successive arrivals (known as a Miles in Trail (MIT) restriction). It is worth noting that the use of runway 11 is often with a slight tailwind component, as the southerly prevailing winds are from 210° to 270° . Above a certain threshold, this tailwind component can lead to an increased MIT restriction of 20 miles between arrivals to runway 11. Departures on 22R can be operated independently from the two arrival runways if takeoffs begin south of the intersection with runway 11. The subsequent analysis will identify the magnitude of added arrival capacity and its impact on the departure capacity.[4]

The runway configuration 22L|22R is symmetric to 4R|4L, so one could expect the two configurations to have the same capacity. However, the airspace design differs substantially between the two runway configurations: Airspace to the south is less restricted than to the north allowing aircraft to be turned to two different (dispersal) departure headings (215° and 239°) immediately after takeoff from runway 22R. This procedure means the inter-departure spacing requirement is reduced to 6000 ft or when the leading departure becomes airborne (unless the leader is a Heavy or B757). Without multiple departure headings, subsequent departures from runway 4L must be given sufficient spacing to ensure that the 2.5 mile terminal radar separation can be maintained between subsequent departures.[4] Thus, taking airspace design into account, the hypothesis is that runway configuration 22L|22R has a higher departure capacity than 4R|4L.

A. Estimation of Saturation Point and Capacity

The throughput curves look very similar to the ones of Figure 8 and can be found in earlier work.[16] The saturation point, N^* is estimated at 26 for both 22L|22R and 11,22L|22R. The resulting capacity curves can be seen in Figure 12.

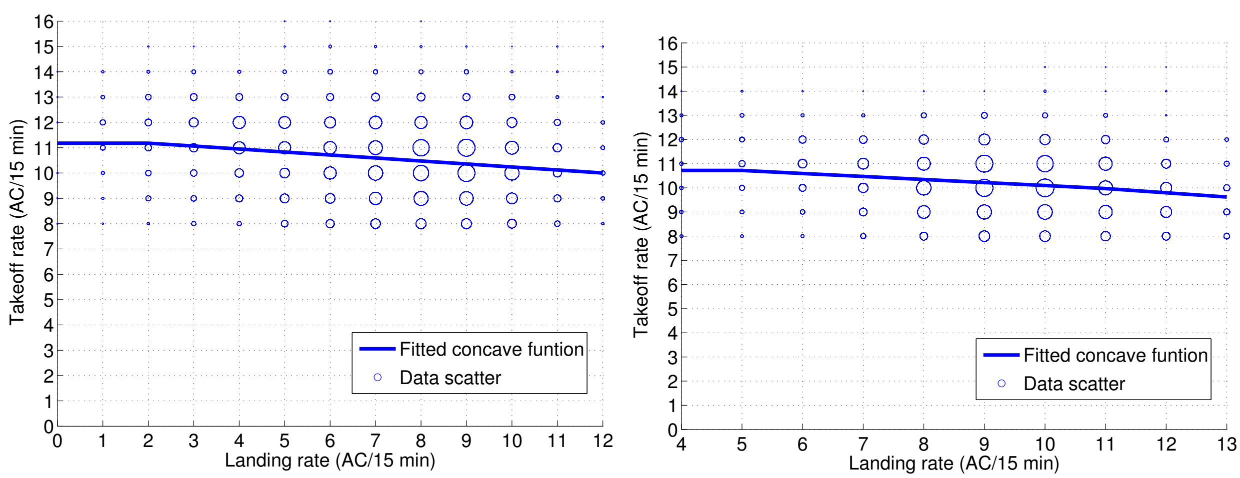

(a) Regression of the takeoff rate as function of landing rate when $N \geq N^*$ for 22L|22R.

(b) Regression of the takeoff rate as function of landing rate when $N \geq N^*$ for 11, 22L|22R.

Figure 12: Capacity curves for the two major south-flow runway configurations.

Comparing Figures 9a, 12a and 12b , we observe:

- Runway configuration (11,22L|22R) tends to be used under high arrival demand. There are hardly any data-points for less than 4 arrivals/ 15 minutes and most of the data-points are found in high arrival counts: between 9 and 12 landings. By contrast, the data-points for runway configuration (22L|22R) are spread across a broad range of arrival counts.

- For arrival counts that can be accommodated by both configurations (4-12 landings/ 15 minutes), the departure capacity of the two configurations is not significantly different. This suggests that the landings on runway 11 do not impact the departures from 22R.
- The addition of runway 11 increases the maximum arrival capacity only by one additional landing. Such a small improvement may be explained by the MIT restrictions that apply to the use of runway 11, and the fact that landings on runway 11 need to be sequenced with runway 22L arrivals.
- The departure capacity of runway configurations 22L|22R and 11,22L|22R is not significantly higher than the departure capacity of the 4R|4L runway configuration, in agreement with the FAA EWR Traffic Management Tips.[8] This finding suggests that, on average, the dispersal headings are not utilized to increase departure capacity. Fleet mix and taxiing-in aircraft crossing the departure runway are potential factors that reduce the effectiveness of the dispersal headings.

B. Impact of Heavy Aircraft Departures

Following the procedure described in Section E, we estimate the impact of Heavy aircraft departures on the departure throughput for the 22L|22R and 11,22L|22R runway configurations. The results of the estimation procedure can be seen in Figure 13.

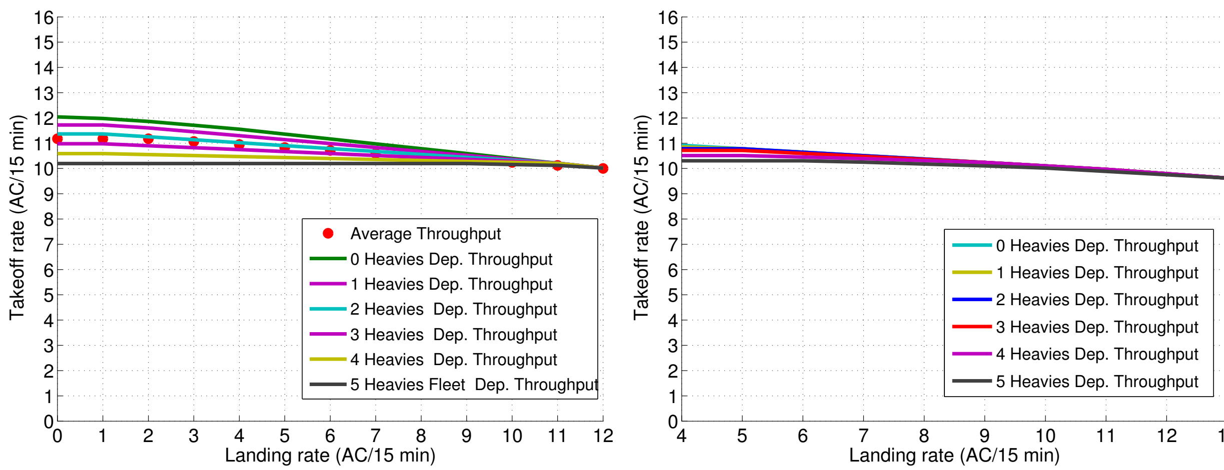

(a) Regression of the takeoff rate as function of landing rate and the number of Heavy departures when $N \geq N^*$ for 22L|22R.

(b) Regression of the takeoff rate as function of landing rate and the number of Heavy departures when $N \geq N^*$ for 11, 22L|22R.

Figure 13: Impact of Heavy aircraft departures for the two major south-flow runway configurations.

From Figure 13a, we note that the departure throughput of the 22L|22R runway configuration increases from 11 takeoffs/15 minutes to 12 takeoffs/15 minutes, given no Heavy departures and a small number of arrivals. This is in contrast to the departure throughput of the 4R|4L configuration, which does not increase substantially with a non-Heavy fleet mix (11a). We hypothesize that the availability of dispersal headings for takeoffs from runway 22R explains this difference. From Figure 13b, we observe that the departure throughput of the 11,22L|22R configuration does not vary significantly with the number of Heavy aircraft in the fleet mix. This can be explained by the high arrival rate served by this runway configuration. Controllers most probably use the large separation requirement between a Heavy and a subsequent departure to have arrivals cross the departure runway. For the same reason the throughput curves of Figure 13a converge as the number of arrivals increases for the 22L|22R configuration as well.

C. Impact of Heavy Aircraft Arrivals

Finally, we estimate the impact of Heavy aircraft arrivals in the south flow runway configurations. The results can be seen in Figure 14. Heavy aircraft arrivals impact both south-flow runway configurations in the same fashion in the common range of arrival rates (4-12 arrivals/ 15 minutes). At a low number of arrivals, two Heavy arrivals come approximately at the cost of one takeoff. The effect of Heavy arrivals diminishes as the total number of arrivals increases. This is similar to the impact of Heavy aircraft arrivals on departure throughput for the 4R|4L configuration (Figure 11b). Finally, the estimated curves in Figures 11b and 14b, and other statistical analysis tools (multiple linear regression, regression trees, random forests) suggest that for both runway configurations (4R|4L and 11,22L|22R), Heavy arrivals impact the departure throughput more significantly than Heavy departures.

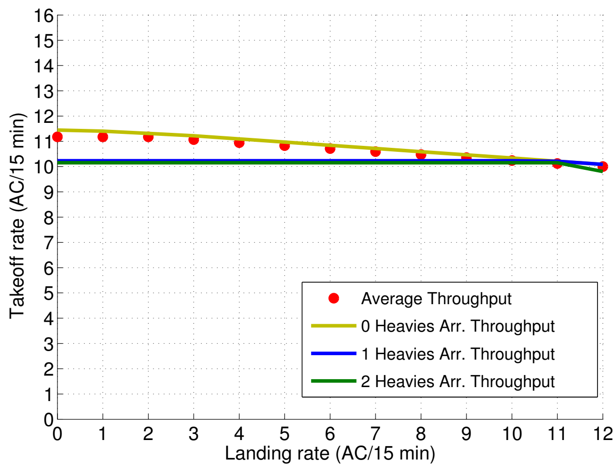

(a) Regression of the takeoff rate as function of landing rate and the number of Heavies landing when $N \geq N^*$ for 22L|22R.

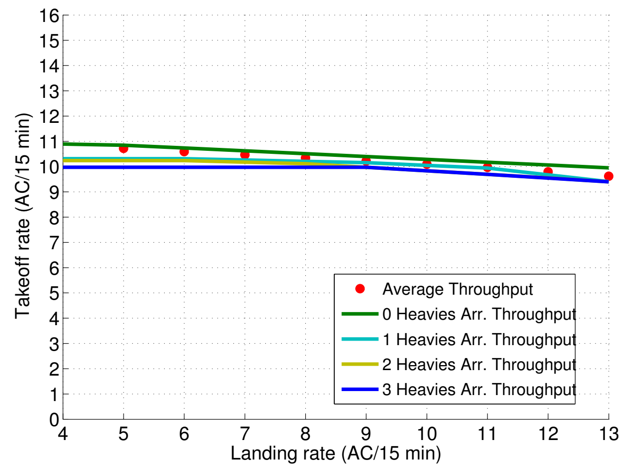

(b) Regression of the takeoff rate as function of landing rate and the number of Heavies landing when $N \geq N^*$ for 11,22L|22R.

Figure 14: Impact of Heavy aircraft arrivals for the two major south-flow runway configurations.

VI. Conclusions and Next Steps

Aircraft size was shown to have an impact on the throughput achievable for several common configurations at EWR. Both Heavy departures and Heavy arrivals have an detrimental impact on the departure throughput for the airport, even when the there are no shared or crossing runways in the reported airport configuration. It was also demonstrated that for two major runway configurations, (4R|4L and 11,22L|22R), Heavy arrivals impact departure throughput more significantly than Heavy departures.

The *average* departure throughput under persistent departure demand of EWR was seen to remain between 9 and 11 takeoffs/15 minutes for a range of runway configurations, airspace designs, arrival capacity and fleet mixes. However, the departure throughput under persistent departure demand also showed very high variance, suggesting that factors not considered by traditional runway capacity models impact airport capacity. Such factors include air traffic flow management programs, human factors, and interactions with the other airports of the New York (NY) metroplex. The methodologies developed in this paper can be extended to investigate some of these factors, and Appendix B presents such an analysis of EWR's interaction with the other major airports in the NY area.

Appendix

A. Correlation between Heavy Departures and Heavy Arrivals

In Sections IV and V, we separately quantified the impact of Heavy arrivals and Heavy departures by estimating the takeoff rate, first as a function of arrivals and Heavy departures, and then as a function of arrivals and Heavy arrivals. In other words, the curves of Figure 11a regress the take-off rate on arrivals and Heavy departures neglecting the impact of Heavy arrivals. For interpreting the results of this regression, it is essential to investigate potential correlation between the Heavy departures and the omitted variable, the Heavy arrivals. For example, if zero Heavy departures are highly correlated with zero Heavy arrivals, then the curves “0 Heavies Departure Throughput” of Figure 11a and “0 Heavies Arrival Throughput” of Figure 11b will be estimating the same quantity, namely, the takeoff rate as a function of the arrival count, conditioned on zero Heavy departures or arrivals.

We therefore perform a simple analysis to test for correlations between the two variables, “Heavy departures” and “Heavy arrivals”. In Figure 15, we plot the number of Heavy departures and the number of Heavy arrivals as a scatter plot for the three major runway configurations at EWR.

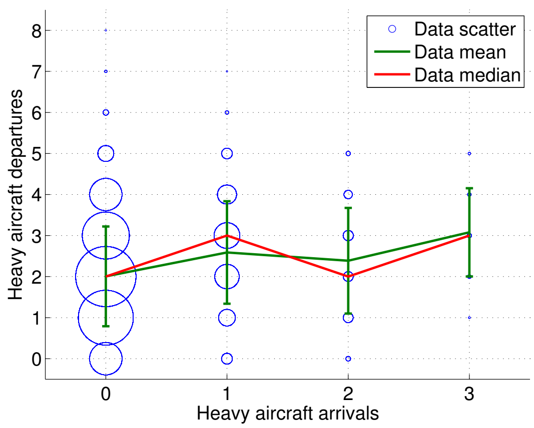

(a) Heavy departures as a function Heavy arrivals at runway configuration (4R | 4L) when $N \geq N^*$

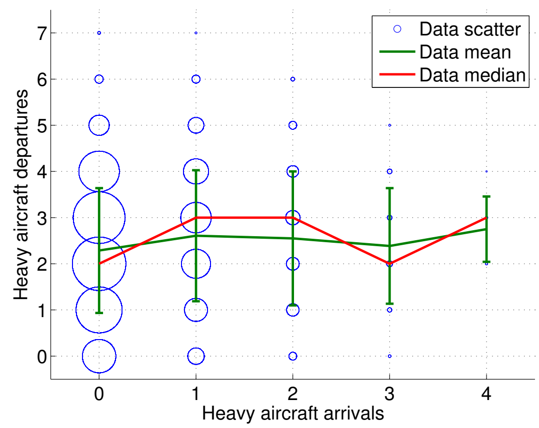

(b) Heavy departures as a function Heavy arrivals at runway configuration (22L | 22R) when $N \geq N^*$

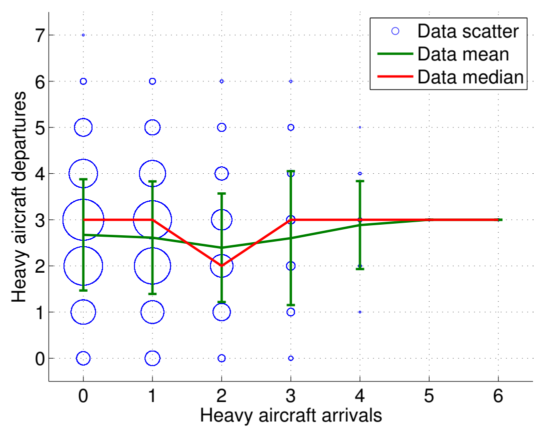

(c) Heavy departures as a function Heavy arrivals at runway configuration (11, 22L | 22R) when $N \geq N^*$

Figure 15: Relation between Heavy departures and Heavy arrivals at three major runway configurations of EWR

We also show the mean and median value of Heavy departures conditioned on the number of Heavy arrivals. The error bars represent one standard deviation of the distribution of Heavy departures conditioned on the number of Heavy arrivals. From these plots, we first note that there is no trend between Heavy departures and Heavy arrivals. At all values of Heavy arrivals, there are 2-3 Heavy departures. We also note that the variance of Heavy departures does not change across the range of Heavy arrivals with sufficient data-points, i.e., 0-3 Heavy arrivals. For all values of Heavy departures, the majority of data-points correspond to no Heavy arrivals. This implies that the curves of Figure 11a and Figure 13, in which the Heavy arrivals are neglected, are representative of zero Heavy arrivals because most of the measurements are under this condition.

Similarly, the regression fits of Figure 11b and Figure 14 neglect the impact Heavy departures. As we saw, there is no correlation between Heavy departures and Heavy arrivals, so neglecting the Heavy departures does not introduce omitted-variable bias in the fits. In addition, for all values of Heavy arrivals, the observations of Heavy departures are more more evenly spread in the range of 1-4 Heavy departures. The fits of Figure 11b and Figure 14 are therefore representative over a range of values of Heavy departures, and are not biased towards a particular value of Heavy departures. Table 4 also presents the correlation between the two variables for the three major configurations.

Table 4: Correlation between Heavy aircraft departures and Heavy aircraft arrivals.

Runway configuration	Correlation between Heavy Departures and Heavy Arrivals
4R|4L	0.1609
22L|22R	0.0854
11,22L|22R	-0.0531

B. Interactions with Other Airports

In prior work, it was conjectured that the capacity of EWR is not fully materialized due to interactions with the other airports in the New York metroplex.[4] In this current study, it was shown that the departure capacity is relatively insensitive to variables that theoretical models suggest being very influential, such as the departing aircraft fleet mix. Examples demonstrated in this study included the observations that departure capacity does not decrease substantially with increasing the number of Heavies in the departures mix, and that it does not reach 15 departures/15 minutes given zero Heavies departures and a small number of arrivals. In addition, when comparing the 4R|4L and 22L|22R configurations, we saw that the availability of dispersal headings in the latter configuration does not translate to a significantly higher capacity. These results motivate an investigation of EWR's interactions with the other two major airports of the New York metroplex, New York John F. Kennedy International Airport (JFK) and New York LaGuardia Airport (LGA). In particular, we would like to see if these interactions explain some of the variation of EWR's departure capacity.

1. *Interactions between JFK and EWR*

As a first step, we study the impact of JFK departures on EWR departures, to see if there is a tradeoff between the "output" of the two airports. This tradeoff could be caused by merging traffic at departure gates or by TRACON workload constraints.[4] In Figure 16, we show the scatter plot of the takeoff rate of EWR in saturation (i.e., under persistent demand) and the takeoff rate of JFK for the three major runway configurations at EWR. We also show the mean and median trend of the EWR takeoff rate in saturation conditioned on the number of takeoffs at JFK.

From Figure 16, we observe that there is no trend indicating that JFK departures negatively impact EWR departure capacity. Instead, the plots suggest a positive trend, which is most pronounced for the 22L|22R configuration. The more efficient JFK is, the more efficient EWR is as well. This positive correlation could be explained by the airspace design, which keeps the departure flows out of the two airports sufficiently

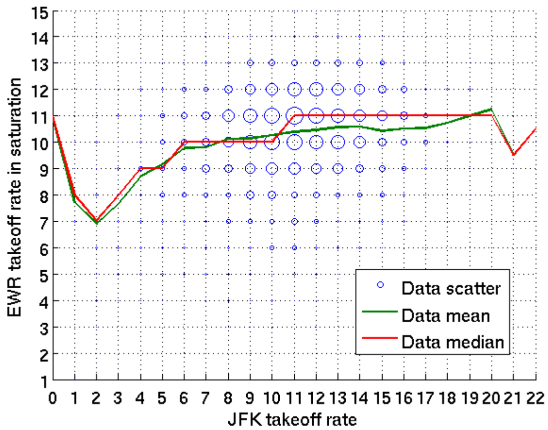

(a) EWR departure capacity as a function of JFK departures for 4R|4L EWR configuration.

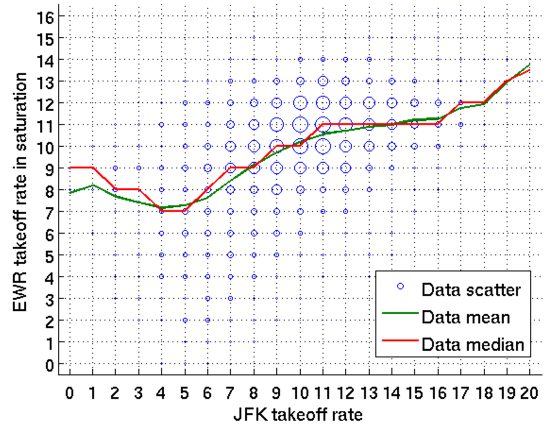

(b) EWR departure capacity as a function of JFK departures for 22L|22R EWR configuration.

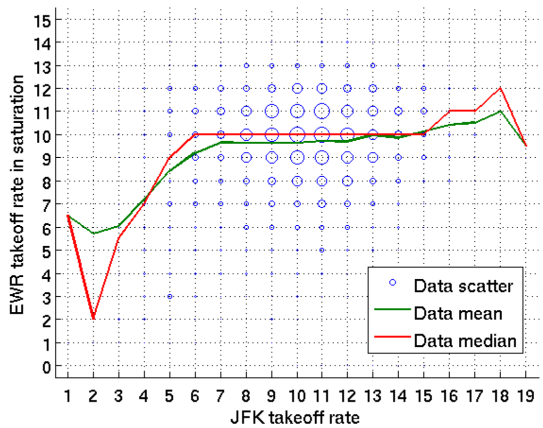

(c) EWR departure capacity as a function of JFK departures for 11,22L|22R EWR configuration.

Figure 16: Relation between EWR departure capacity and JFK departures for three major runway configurations of EWR.

separated. Thus, the "output" of JFK does not negatively impact the "output" of EWR. However, when comparing Figures 16b and 16a, we note that the EWR mean takeoff rate does not exceed 11 operations/15 minutes for all values of JFK departures in the 4R|4L configuration. However, in the 22L|22R configuration, the mean takeoff rates at EWR exceed 11 operations/15 minutes for high values of JFK departures. This suggests that when JFK throughput is very high, EWR throughput increases as well, for the 22L|22R configuration. High JFK departure throughput implies good route availability in the New York airspace, which, in turn, could imply good route availability for EWR departures. Because the airspace to the south of EWR is not constrained, departures make use of the increased routing options and increase their throughput. However, when the airport operates in the 4R|4L configuration, the departure throughput cannot increase as much because of airspace constraints.

In order to further investigate the correlation of the departure capacity of the two airports we restrict the data-points for the takeoff rate at JFK to the ones under persistent demand (in saturation). In Figure 17, we show the scatter plot of the takeoff rate of EWR in saturation (i.e. under persistent demand) and the takeoff rate of JFK in saturation (i.e. under persistent demand) for the three major runway configurations at EWR. We also show the mean and median trend of the EWR takeoff rate in saturation, conditioned on the takeoff rate of JFK in saturation.

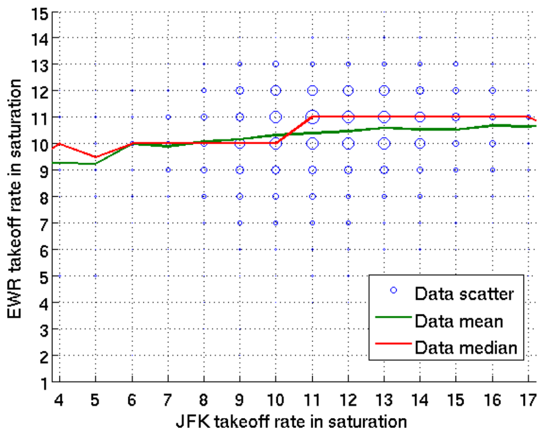

(a) EWR departure capacity as a function of JFK departure capacity for 4R|4L EWR configuration.

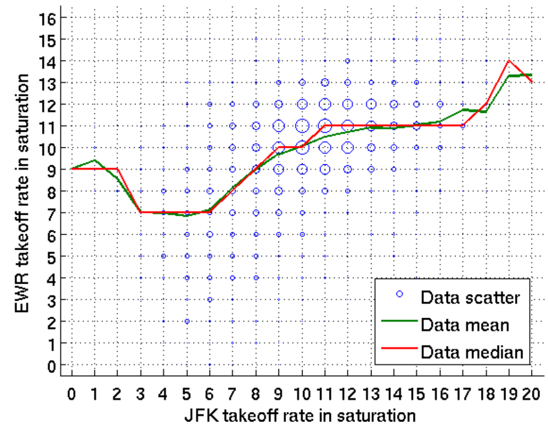

(b) EWR departure capacity as a function of JFK departure capacity for 22L|22R EWR configuration.

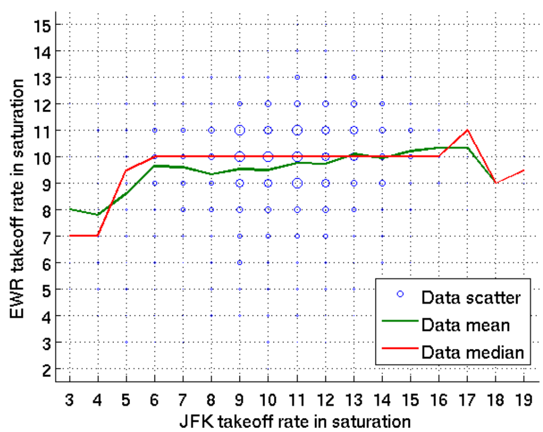

(c) EWR departure capacity as a function of JFK departure capacity for 11,22L|22R EWR configuration.

Figure 17: Relation between EWR departure capacity and JFK departure capacity for three major runway configurations of EWR.

The plots of Figure 16 and Figure 17 are quite similar, suggesting that JFK departures interact with EWR departures in the same way irrespective of whether or not JFK is saturated. The positive correlation between EWR and JFK capacity suggests the presence of hidden variables which impact the departure capacity of the two airports in a similar fashion. One such factor could be the arrivals: When the one airport experiences an arrival push, the other airport is likely to experience one as well. Similarly, both airports experience a large number of Heavy aircraft departures in the evening. Another factor could be downstream weather, or route availability. We note that when the takeoff rate of JFK is very low (fewer than 7 departures per 15 minutes), the takeoff rate of EWR is low as well. Given that both airports are under persistent departure demand and both have very low departure throughput, it is possible that downstream constraints keep both airports at low performance.

To further emphasize the correlation between EWR and JFK takeoff rates under persistent demand, we compare the correlation coefficient between the two to the correlation coefficient between EWR takeoff rate in saturation and EWR landing rate, in Table 5. We note the correlation between the departure capacity of the two airports is higher, in absolute values, than the correlation between the departure capacity of EWR and the arrival capacity of EWR for two out of the three major configurations. This preliminary analysis shows no evidence that JFK departures impact negatively EWR departures.

Table 5: Correlation between EWR departure capacity and JFK departure capacity.

EWR runway configuration	Correlation between EWR dep. capacity and JFK dep. capacity	Correlation between EWR dep. capacity and EWR arr. capacity
(4R | 4L)	0.1417	-0.2608
(22L | 22R)	0.4739	-0.0529
(11, 22L | 22R)	0.1378	-0.0816

2. *Metroplex Local Regression*

In this Section, we generalize the results of the previous section. Following the method outlined in earlier work,[4] we treat the whole metroplex as a single airport system of which EWR is one component. The most frequently used runway configuration in the metroplex in 2007 is the "South-Flow-VMC-Arrival Priority", described in Table 6. For all runway configurations comprising "South-Flow-VMC-Arrival Priority", we calculate the saturation point using the methodology of Section IV. We now keep all data points for which the metroplex is in "South-Flow-VMC-Arrival Priority" and all individual airports are in saturation ($N \geq N^*$). We study the interactions among the following variables:

1. Departures_1: Departure throughput in each 15-minute time interval at JFK
2. Arrivals_1: Arrival throughput in the 15-minute interval at JFK
3. Departures_2: Departure throughput in the 15-minute time interval at EWR
4. Arrivals_2: Arrival throughput in the 15-minute interval at EWR
5. Departures_3: Departure throughput in the 15-minute interval at LGA
6. Arrivals_3: Arrival throughput in the 15-minute interval at LGA

Table 6: Components of the "South-Flow-VMC-Arrival Priority" metroplex configuration.

Airport	Arrival Runway(s)	Departure Runway	Weather	N^*
JFK	13L, 22L	13R	VMC	24
EWR	11, 22L	22R	VMC	26
LGA	22	13	VMC	11

As was done in Section D, we analyze the correlations between all the variables using the *pairs* function of the R programming language which produces panels with the correlations among all variables of the model. Each panel of Figure 18 shows the scatterplot between the variable on the vertical axis and the variable on the horizontal axis as well as the lowess curve (in red) through a set of data points. From the lowess fit lines, we observe that there is no negative correlation between departures out of one airport of the Metroplex and operations at another airport. On the contrary, we note the decreasing trend between Departures_i and Arrivals_i resulting from the shared capacity between departures and arrivals at each individual airport (the capacity envelope). We also note the increasing trend between Departures_2 and Arrivals_2 suggesting a positive correlation between the departure capacity of EWR and LGA. This observation is consistent with analysis of Section 1, which showed a positive correlation between the Departure capacity of EWR and JFK. These results were verified using other statistical models, as well, such as generalized additive models, regression trees, and random forests. In conclusion, the analysis of the metroplex configuration "South-Flow-VMC-Arrival Priority" shows that the departure capacity of each airport does not depend on operations at other airports.

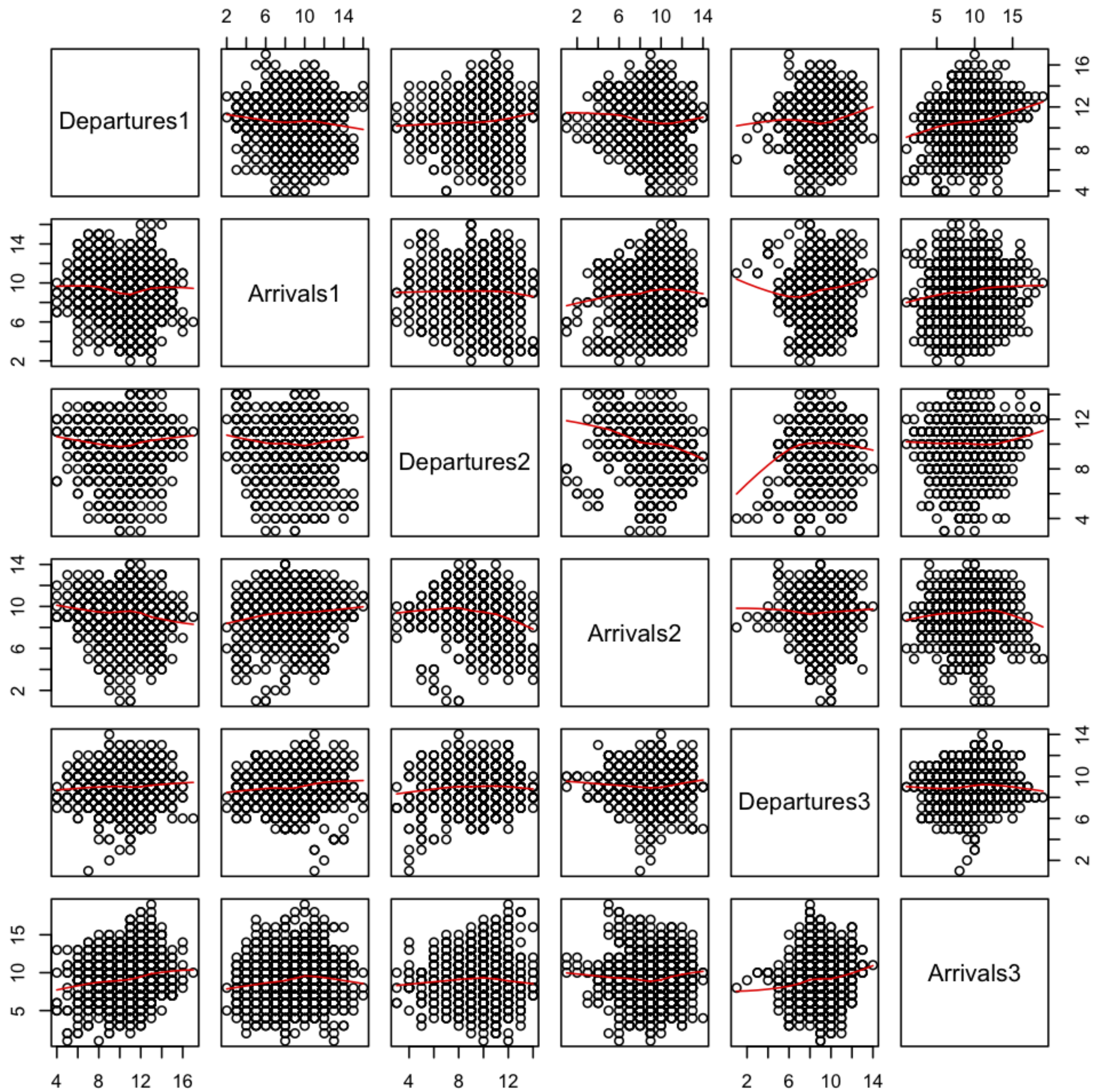

Figure 18: Correlations between departures and arrivals at the New York metroplex for the "South-Flow-VMC-Arrival Priority" configuration.

References

[1] J. Cohen. *Applied multiple regression/correlation analysis for the behavioral sciences*. Lawrence Erlbaum, 2003.

[2] R. De Neufville and A.R. Odoni. *Airport systems: Planning, design, and management*. McGraw-Hill Professional, 2002.

[3] Richard de Neufville and Amedeo Odoni. *Airport Systems: Planning, Design and Management*. McGraw-Hill, 2003.

[4] A. D. Donaldson and R.J. Hansman. Improvement of terminal area capacity in the New York airspace. Technical report, Massachusetts Institute of Technology, 2011. No. ICAT-2011-4.

[5] Federal Aviation Administration. *Order JO 7110.65S - Air Traffic Control*. U.S. Department of Transportation, February 2008.

[6] Federal Aviation Administration. Aircraft characteristics database. http://www.faa.gov/airports/engineering/aircraft_char_database, December 2009.

[7] Federal Aviation Administration. Aviation System Performance Metrics database. http://aspm.faa.gov/aspm/ASPMframe.asp, February 2010.

[8] Federal Aviation Administration. EWR traffic management tips. http://www.fly.faa.gov/Information/east/zny/ewr/ewr_tm.htm, February 2010.

[9] Federal Aviation Administration. JO 7110.541 Interim Procedures for Airbus A388 Flights, October 2010.

[10] E. P. Gilbo. Airport capacity: Representation, estimation, optimization. *IEEE Transactions on Control Systems Technology*, 1(3):144–154, 1993.

[11] M. Grant and S. Boyd. Graph implementations for nonsmooth convex programs. In V. Blondel, S. Boyd, and H. Kimura, editors, *Recent Advances in Learning and Control*, Lecture Notes in Control and Information Sciences, pages 95–110. Springer-Verlag Limited, 2008. http://stanford.edu/~boyd/graph_dcp.html.

[12] M. Grant and S. Boyd. CVX: Matlab software for disciplined convex programming, version 1.21. http://cvxr.com/cvx, April 2011.

[13] MITRE Corporation and Federal Aviation Administration. Airport capacity benchmark report 2004. Technical report, 2004.

[14] Nikolaos Pyrgiotis. *A Stochastic and Dynamic Model of Delay Propagation Within an Airport Network For Policy Analysis*. PhD thesis, Massachusetts Institute of Technology, 2011.

[15] V. Ramanujam and H. Balakrishnan. Estimation of Arrival-Departure Capacity Tradeoffs in Multi-Airport Systems. In *Proceedings of the 48th IEEE Conference on Decision Control*, 2009.

[16] I. Simaiakis. Modeling and control of airport departure processes for emissions reduction. Master's thesis, Massachusetts Institute of Technology, 2009.

[17] I. Simaiakis and H. Balakrishnan. Departure throughput study for Boston Logan International Airport. Technical report, Massachusetts Institute of Technology, 2011. No. ICAT-2011-1.